Band Structures of and Bonding in 10-Electron Solids: MnAl, CrSi, VP, TiS

R. J. Kematick and C. E. Myers*

Department of Chemistry and Materials Research Center, Binghamton University (SUNY), P.O. Box 6000, Binghamton, New York 13902-6000

Received March 6, 1992

The electronic structures of the 10-electron series of binary MX compounds MnAl–CrSi–VP–TiS have been investigated using an extended Hückel calculational approach. The results, particularly the variations of overlap population in the different bonds, help provide an understanding of the changes in atomization enthalpy and crystal structure across the series. The calculations show a change in the manner in which the p-block element uses its s-electrons in bonding, and this change correlates with a change in preferred crystal structure. In TiS and VP, with the NiAs-type structure, the bonding is dominated by M–X interactions, whereas, in CrSi and MnAl which have different structures, X–X interactions are of increasing importance.

Introduction

The research described here is part of a broad study of compounds of first-row transition metals with p-block elements. Among the goals of this program are acquisition of reliable thermodynamic data for those systems for which such data are lacking, documentation of stability trends, and development of an understanding of these trends in terms of atomic properties and concepts of chemical bonding. This paper is concerned with the last of these goals. The current focus is on an isoelectronic series of 1:1 compounds with 10 valence electrons, namely "MnAl", CrSi, VP, and TiS. Whereas the last three of these substances are stoichiometric compounds with narrow ranges of homogeneity, "MnAl" (hereinafter referred to simply as MnAl) does not form at a unique stoichiometry, but rather as a solid solution in the γ single-phase region.[1] Both TiS and VP are found in the NiAs-type structure[2] but exhibit large c/a ratios which suggests relatively small metal–metal interaction in the c-direction in these solids. CrSi has the FeSi-type structure[2] and the γ form of MnAl has a body-centered cubic structure which may be considered a disordered CsCl-type structure.[3]

In Figure 1 the enthalpies of atomization of MX (where M is a transition metal and X a p-block element) compounds to ground-state atoms are plotted as a function of the number of valence electrons per MX pair.† This graph includes first-row transition-metal sulfides, phosphides, silicides, and aluminides. For the 10-electron compounds, the order is VP > TiS > CrSi > MnAl. The enthalpy of atomization, which is approximately the same as the cohesive energy, may be viewed as the difference in the total electron energy in the MX solid and in the isolated ground-state atoms. A commonly employed scheme for analyzing cohesive energies of solids involves the invocation of a cycle in which the ground-state atoms are promoted to a valence-state configuration which maximizes the number of unpaired electrons, and then the valence-state atoms bond to form a solid. The valence-state energy may be taken as the average energy of the valence-state configuration which can be calculated from spectroscopic data.[4] The atomization energy to the valence-state atoms might then be expected to be a smooth function of the number and type of bonding electrons and effective nuclear charge.

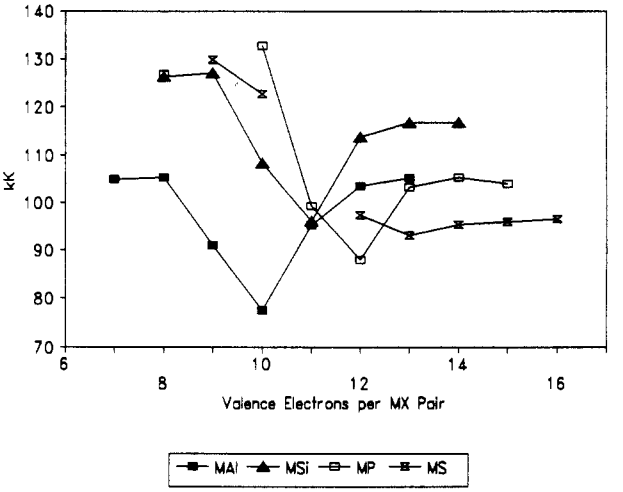

Figure 1. Enthalpies of atomization of MX(s) compounds.

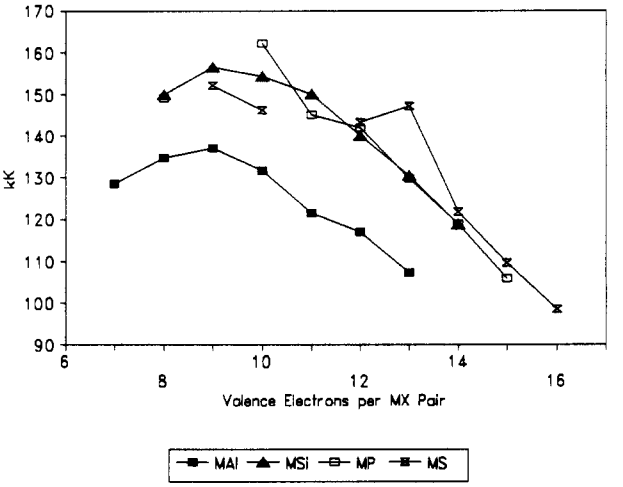

Figure 2. Enthalpies of atomization of MX(s) compounds to valence-state metal atoms.

The atomization enthalpies to hypothetical valence-state metal atoms[5] are shown in Figure 2, where the transition metal is assumed to have the $d^{n-1}s$ configuration and the corresponding

† Energy units are in kilokelvins (kK); energies in other units may be obtained upon multiplication by the appropriate value of the gas constant R.

(1) McAlister, A. J.; Murray, J. L. *Bull. Alloy Phase Diagrams* **1987**, *8*, 438.
(2) Villars, P.; Calvert, L. D. *Pearson's Handbook of Crystallographic Data for Intermediate Phases*; American Society for Metals: Metals Park, OH, 1985.
(3) Ellner, M. *Metall. Trans. A* **1990**, *21A*, 1669.
(4) Slater, J. C. *Quantum Theory of Atomic Structure*; McGraw-Hill: New York, 1960; Vols I and II.
(5) Myers, C. E. *High Temperature Materials Chemistry—IV*, Munir, Z. A., Cubicciotti, D., Eds.; Electrochemical Society: Pennington: NJ, 1988; Proceedings Vol. 88-5, p 584.

0020-1669/92/1331-3568$03.00/0

valence-state energies[6] have been added to the respective atomization enthalpies. The order for the 10-electron compounds is now VP > CrSi > TiS > MnAl. The agreement among the sulfides, phosphides, and silicides for 11 electrons and more is remarkable; MnS exhibits the only major difference, and it has been shown[7] to be significantly ionic. It should be noted, however, that valence-state energies for the p-elements have not been included in Figure 2. The valence-state energies for aluminum and silicon would include a significant promotion energy, assuming sp^2 and sp^3 valence states. Thus if p-element valence-state energies are added, the sulfide and phosphide points are increased only by 3.5 and 8.2 kK, respectively, but the silicides are increased by 73.2 and the aluminides by 59.0 kK. The silicide and aluminide data sets would then fall significantly above those of the sulfides and phosphides. These observations lead to a number of questions. Inasmuch as mixing of electronic configurations is to be expected in the formation of energy bands in the solid, to what extent are the hypothetical valence states (which assume no mixing of configurations) correct or reasonable for the metals in Figure 2? To what extent do Al and Si s-electrons participate in the bonding? What factors are responsible for the trend observed in the atomization enthalpies? What is the role of the crystal structure and the arrangement and distances of nearest neighbors? It was in seeking answers to these questions that an extended Hückel (EH) approach to the calculation of band structures was initiated. Although care should be exercised in attempting to draw quantitative conclusions, the EH method does provide useful insights into the basis for trends in structure and bonding. The existence of a band structure calculation on TiS at the KKR level of approximation[8] affords a useful comparison. In addition, Pettifor and Podloucky[9] have applied a tight-binding model to examine the relative stabilities of the crystal structures of pd-bonded AB compounds. Their approach, which neglected the s-electrons, was applied to mapping of structures in terms of an electronegativity scale and the numbers of p- and d-electrons and accounted qualitatively for the observed domains of the NaCl, CsCl, NiAs, MnP, FeB, and CrB structure types, but not for the FeSi structure type.

Calculation

The energy band structures of MnAl, CrSi, VP, and TiS were calculated by the extended Hückel method as developed by Whangbo and Hoffmann.[10] Among the necessary input parameters are Slater-type orbital exponents for the various atomic orbitals used to construct the crystal wavefunctions and Coulomb integral values (H_{ii}) for the atomic levels. The H_{ii} values depend on the electronic configuration and charge of the atom in question, and in the case of fractional occupancy of atomic orbitals, it is necessary to take linear combinations of free atom electron configurations in evaluating H_{ii}s. A charge iterative procedure was thus used in these calculations to determine H_{ii} values consistent with the results of a Mulliken type population analysis of the occupied crystal states.[11] The iterations were continued until the number of s-, p-, and d-electrons on each atom changed by less than 0.02 electrons from input to output on a single cycle. For the elements Al, Si, P, and S the orbital exponents used in the calculations were taken from Clementi and Roetti[12] and the needed charge iteration parameters from Cusachs.[13] Charge iteration parameters for the transition metals Mn, Cr, V, and Ti were taken from tables of Basche, Viste, and Gray[14] and orbital exponents from Richardson et al.[15] Crystallographic data[2] for the compounds under study are summarized in Table I. MnAl was constructed in a primitive cubic CsCl-type cell, CrSi was constructed in a primitive cubic FeSi cell, and VP and TiS were constructed in primitive hexagonal NiAs cells. The calculations for the cubic structures were performed at 56 "**k** points" in the irreducible $^1/_{48}$th of the cubic Brillouin zone. For the hexagonal structures 45 **k** points were taken from $^1/_{24}$th of the hexagonal Brillouin zone. In calculation of the density of states curves by a histogram technique, each **k** vector was given a weight proportional to the number of vectors in the star of that **k** vector.

Table I. Structural Data

	MnAl		
type = CsCl	cubic ($Pm3m$)		a = 3.050 Å
	atomic positions		
Mn	0.0	0.0	0.0
Al	0.5	0.5	0.5
	CrSi		
type = FeSi	cubic ($P2_13$)		a = 4.607 Å
	atomic positions		
Cr	0.136	0.136	0.136
Cr	0.636	0.364	0.864
Cr	0.864	0.636	0.364
Cr	0.364	0.864	0.636
Si	0.846	0.846	0.846
Si	0.346	0.654	0.154
Si	0.154	0.346	0.654
Si	0.654	0.154	0.346
	VP		
type = NiAs	hexagonal ($P6_3/mmc$)	a = 3.180 Å	c = 6.224 Å
	atomic positions		
V	0.0	0.0	0.0
V	0.0	0.0	0.5
P	0.333	0.667	0.250
P	0.667	0.333	0.750
	TiS		
type = NiAs	hexagonal ($P6_3/mmc$)	a = 3.299 Å	c = 6.380 Å
	atomic positions		
Ti	0.0	0.0	0.0
Ti	0.0	0.0	0.5
S	0.333	0.667	0.250
S	0.667	0.333	0.750

The results of the calculations included density of state (DOS) and l-decomposed DOS (LD-DOS) curves. The overlap populations[16] for each symmetry-unique bond (with bond lengths less than 3.5 Å) in each compound were also computed. Since a goal of this study is an intercomparison of the relative contributions of the M–M, M–X, and X–X bonding interactions in the target compounds, we have chosen to present curves which display the total overlap population (per primitive cell) for these interactions as a function of energy. These curves were constructed by summing over the symmetry-unique bonds, giving each bond a weight determined by the coordination geometry of the crystal. As an example, in the CrSi (FeSi) structure, each Cr atom is surrounded by seven Si atoms, one at a distance of 2.314 Å (I), three at 2.423 Å (II), and three more at 2.576 Å (III). The total Cr–Si overlap population would thus be POP(I) + 3POP(II) + 3POP(III).

(6) Griffith, J. S. *J. Inorg. Nucl. Chem.* **1956**, *3*, 15.
(7) Franzen, H.; Sterner, C. *J. Solid State Chem.* **1978**, *25*, 227.
(8) Nakahara, J.; Franzen, H.; Meismer, D. K. *J. Chem. Phys.* **1982**, *76*, 4080.
(9) (a) Pettifor, D. G.; Podloucky, R. *Phys. Rev. Lett.* **1984**, *53*, 1080. (b) Pettifor, D. G.; Podloucky, R. *J. Phys. C: Solid State Phys.* **1986**, *19*, 315.
(10) (a) Whangbo, M.-H.; Hoffmann, R. *J. Am. Chem. Soc.* **1978**, *100*, 6093. (b) Hoffmann, R. *Solids and Surfaces: A Chemists View of Bonding in Extended Structures*; VCH Publishers: New York, 1988.
(11) McGlynn, S. P.; VanQuickenburg, L. G.; Kinoshita, M.; Carroll, D. G. *Introduction To Applied Quantum Chemistry*; Holt Rinehart and Winston: New York, 1972.
(12) Clementi, E.; Roetti, C. *At. Nucl. Data Tables* **1974**, *14*, 177.
(13) Cusachs, L. C.; Reynolds, J. W. *J. Chem. Phys.* **1965**, *43*, 160S.
(14) Basche, H.; Viste, A.; Gray, H. B. *Theor. Chim. Acta* **1965**, *3*, 458.
(15) Richardson, J. W.; Nieuwport, W. C.; Powell, R. R.; Edgell, W. F. *J. Chem. Phys.* **1962**, *36*, 1057.
(16) Hughbanks, T.; Hoffmann, R. *J. Am. Chem. Soc.* **1983**, *105*, 3529.

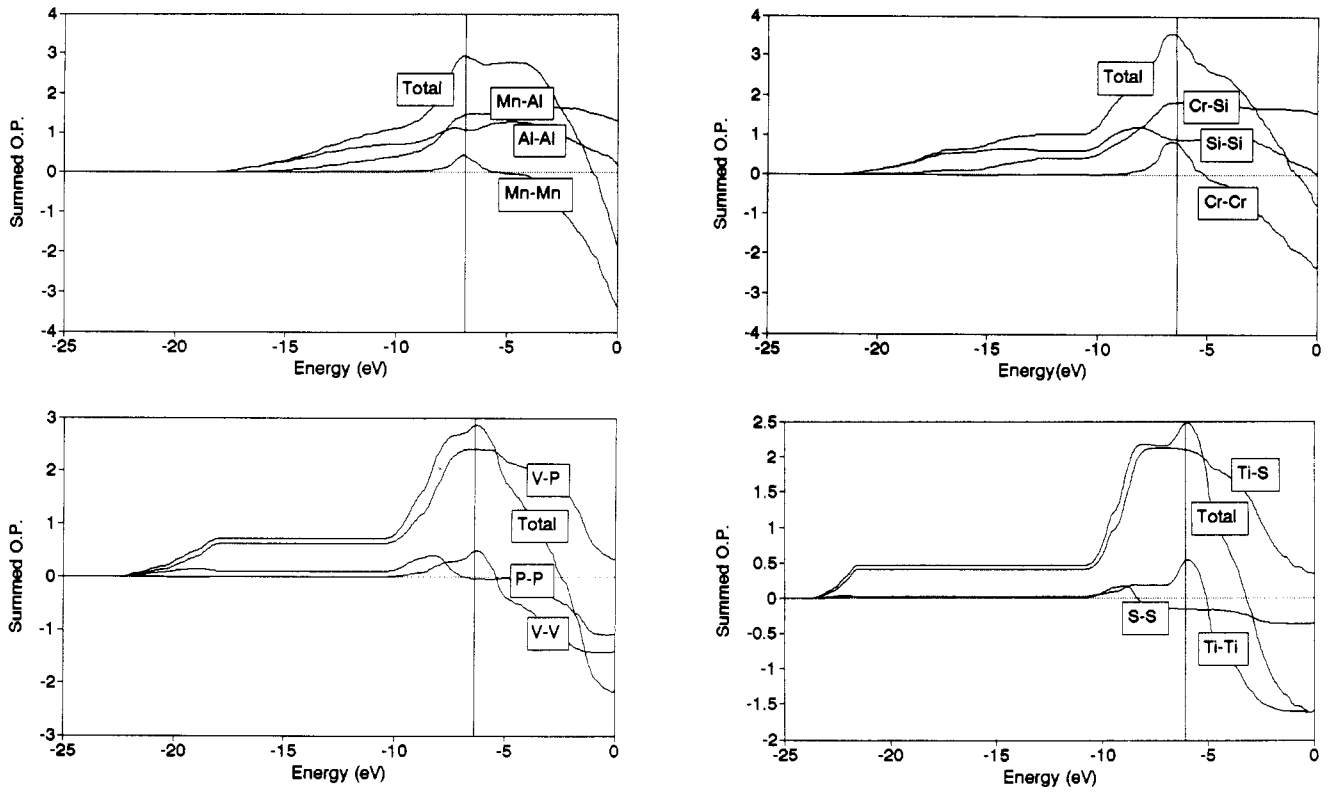

Figure 3. Summed overlap population curves for bond types (a, top left) MnAl in the CsCl-type structure, (b, top right) CrSi in the FeSi-type structure, (c, botton left) VP in the NiAs-type structure, and (d, bottom right) TiS in the NiAs-type structure.

In the extended Hückel method, the total valence electron energy of the solid is approximated by the sum of the single-electron energy eigenvalues over all occupied levels (i.e. all **k** points and all $E < E(\text{Fermi})$). A similar approximation is made for the isolated atoms, and the cohesive energy obtained from the difference.

Results and Discussion

The DOS and LD-DOS curves for the series of compounds MnAl–CrSi–VP–TiS are available in the supplementary material. The features of these curves change somewhat systematically across the series. To a good approximation, the total DOS can in all cases be reconstructed as a sum of the p-element s,p-states and transition-element d-states. The DOS of MnAl shows no valence-conduction band separation and is dominated by Mn d-type contributions. A rather free electron-like band primarily of Al s-character forms at low energy, and there is some Al p-contribution to the conduction band. In CrSi a gap begins to form between the conduction band and a low-lying set of states predominantly of Si s-character. The conduction band is again dominated by Cr d-states with some Si p-states. In VP the P s-band has shifted to still lower energy and has narrowed, and the P p-levels have begun to drop from the conduction band. In TiS the non-metal (S) p-states have separated from the conduction band completely, and the S s-states form a still narrower low-lying band. The total and partial densities of states for TiS from this EH calculation are essentially the same as those from KKR calculations[8] for the conduction and valence bands, but the sulfur s-band from the EH calculation lies significantly lower than in the KKR case.

The observed shifting of the p-element levels to progressively lower energy across the series MnAl–CrSi–VP–TiS is expected because of the increasing atomic number on the p-element. The s-orbitals on the p-element also become more spatially contracted. Conversely, on the basis of the decreasing atomic number on the transition metal across the series, the transition-metal d-orbitals become somewhat more extended. One might thus expect that overlap between the p-element s-orbitals and transition-metal d-orbitals would become more effective across the series, resulting in higher net M–X overlap and stronger M–X bonds.

Table II. Average Overlap Populations for the Unique Bond Types (Evaluated at the Fermi Level)

N^a	bond type	bond distance (Å)	OP[b]
8	Mn–Al	2.614	0.183
6	Al–Al	3.050	0.177
6	Mn–Mn	3.050	0.067
6	Si–Si	2.846	0.147
6	Cr–Cr	2.824	0.130
1	Cr–Si(1)	2.314	0.353
3	Cr–Si(2)	2.423	0.302
3	Cr–Si(3)	2.576	0.190
	Cr–Si(av)	2.473	0.261
6	P–P	3.180	–0.006
6	V–P	2.407	0.401
2	V–V (*c*-axis)	3.112	0.064
6	V–V (planar)	3.180	0.060
6	S–S	3.299	–0.025
6	Ti–S	2.484	0.349
2	Ti–Ti (*c*-axis)	3.190	0.055
6	Ti–Ti (planar)	3.299	0.069

[a] N is the number of equivalent bonds at each unique distance. [b] OP is the overlap population.

The overlap population curves (weighted sums over symmetry-unique bonds) are presented in Figure 3, and the average overlap populations for the symmetry-unique bonds are presented in Table II. A significant variation in the relative contribution of the different bond types (M–X, M–M, X–X) to the total overlap population is indeed observed as one traverses the series MnAl–CrSi–VP–TiS. In MnAl the lowest energy interactions are seen to be Al–Al (X–X) type, and at the Fermi level position the Al–Al and Mn–Al bond orders are comparable. In CrSi the lowest energy interactions are still Si–Si (X–X) type, but at the Fermi level the Cr–Si interactions have become dominant. MnAl and CrSi contrast sharply with the NiAs-type compounds VP and TiS. The MX type interactions begin to occur at lower energies and contribute most heavily to the total overlap population

Table III. Extended Hückel Input Parameters and Computed Energies

	H_{ss}[a]	H_{pp}	H_{dd}	ζ_s[b]	ζ_p	ζ_{d1}	ζ_{d2}	C1[c]	C2
				MnAl					
Mn	−6.688	−3.186	−7.03	1.84	1.84	5.15	1.90	0.532	0.649
Al	−12.268	−6.098	1.37	1.36					
E(Fermi) = −6.865 eV									
E(tot) = −85.97 eV									
E(coh) = −11.53 eV									
				CrSi					
Cr	−6.674	−3.108	−6.695	1.7	1.7	4.95	1.80	0.506	0.675
Si	−15.753	−7.334	1.63	1.43					
E(Fermi) = −6.380 eV									
E(tot) = −380.007 eV									
E(coh) = −14.31 eV									
				VP					
V	−6.589	−3.325	−6.46	1.3	1.3	4.75	1.70	0.476	0.705
P	−18.462	−7.638	1.88	1.63					
E(Fermi) = −6.369 eV									
E(tot) = −205.61 eV									
E(coh) = −15.16 eV									
				TiS					
Ti	−6.560	−3.263	−6.158	1.5	1.5	4.55	1.6	0.439	0.740
S	−21.582	−8.469	2.12	1.83					
E(Fermi) = −6.097 eV									
E(tot) = −224.49 eV									
E(coh) = −14.90 eV									

[a] H_{ss}, etc. are the s, p, d coulomb integrals. [b] ζ_s, etc. are the exponents of Slater-type orbitals. [c] C1 and C2 are coefficients of double ζ expansion (d-orbitals).

Table IV. Computed Electron Occupations

MX	M(s)[a]	M(p)	M(d)	X(s)	X(p)	Q(M)[b]	Q(X)
MnAl	0.41	0.23	6.35	1.29	1.71	6.99	3.01
CrSi	0.40	0.39	5.25	1.50	2.47	6.03	3.97
VP	0.52	0.26	4.19	1.65	3.38	4.97	5.03
TiS	0.46	0.41	3.09	1.74	4.30	3.96	6.04

[a] M(s), M(p), and M(d) are the transition-metal s-, p-, and d-orbitals. X(s) and X(p) are the "p-element" s, p-orbitals. [b] Q(M) and Q(X) are the total charge on atoms M or X.

in the NiAs-type structures. In the two NiAs phases the net X–X overlap is negative. Finally, the average overlap population in the M–X bond increases in parallel with the experimental atomization enthalpies shown in Figure 1; i.e. the sequence is MnAl–CrSi–TiS–VP. The cohesive energies as computed from extended Hückel total energies also show this same sequence (Table III).

It is of some interest to examine the extent of M–M bonding in the NiAs-type phases. In an ideal close-packed NiAs structure the c/a ratio is 1.63. Ratios smaller than this ideal ratio are generally taken to be indicative of metallic bonding character (via d_{z^2} interlayer interactions) while larger ratios indicate a more ionic character.[17] The c/a ratio of VP is 1.956 and of TiS is 1.937, and hence one would not expect significant M–M bonding in these compounds. An examination of the data in Table II shows that the in-plane and out-of-plane M–M bonds are of comparable strengths; i.e. the bond along the c-axis is not especially stronger. In fact the M–M bond along the c-axis actually appears weaker in TiS than in VP. An argument based on increasing M–M bonding along the c-axis with decreasing c/a ratio would fail to explain this.

Table IV lists the orbital occupations and total charges on the individual atoms for the compounds being studied. There is little indication of significant ionic character in any of these materials.

In a recent paper, Brewer has analyzed the bonding in transition-metal aluminides.[18] A central argument in this analysis is that the rather diffuse s,p-orbitals on aluminum do not overlap well with the rather localized d-orbitals on the transition metals. On the basis of a consideration of valence-state energies for both aluminum and the transition metals, it was argued that, in the formation of compounds between aluminum and a transition metal, aluminum would retain an s^2p configuration while the transition metal would vacate its s-orbital by assuming either a d^n or $d^{n-1}p$ configuration. The empty transition-metal s-orbital could then overlap with the s^2 pair on aluminum to form an effective bond, more than compensating for any needed promotion energy for the transition metal. Aluminum thus would act as a Lewis base in bonding to a transition metal. An examination of the DOS and OP curves for the case of MnAl shows that the Al s-electrons are, however, involved mostly in Al–Al bonding. A detailed examination of the LD-DOS curves indicates that 100% of the occupied Al s-states lies below an energy of about −10 eV, while only 30% of the occupied Mn s-states falls below this energy. Thus, although a Lewis acid–base interaction between Mn and Al involving s-orbitals on each atom cannot be entirely ruled out, it is unlikely to be a significant bonding effect between Mn and Al.

The involvement of the p-element s-orbitals in the overall bonding clearly changes across the series. Indeed, for MnAl and CrSi the Al and Si s-orbitals are involved mostly in X–X (Al–Al or Si–Si) bonding. In VP and TiS the P and S orbitals are involved mainly in M–X bonding. Between CrSi and VP the net X–X overlap becomes negative (indicating a predominance of X–X antibonding states below the Fermi level), the role of the p-element s-electrons changes, and the crystal structure changes. CrSi occupies a pivotal position in this series and can be taken as a test case in exploring changes in the underlying interactions.

To explore this further, we have performed calculations where CrSi was placed into both the VP unit cell and the MnAl unit cell and compared the computed overlap population curves in the imaginary structure to those in the observed (FeSi) structure. Table V presents values of the average overlap population for the symmetry-unique bonds in each case. Placing CrSi into the VP cell significantly increases the overlap in the Cr–Si bond, while simultaneously weakening the Si–Si and Cr–Cr bonds. Placing CrSi into the MnAl cell results in a slightly reduced overlap

(17) Adams, D. W. *Inorganic Solids*; John Wiley & Sons: New York, 1974.
(18) Brewer, L. *J. Phys. Chem.* **1990**, *94*, 1196.

Table V. Comparison of CrSi Bond Overlaps in Different Structures

N^a	bond type	length		OP[b]
	CrSi in FeSi-Type Structure (Observed Structure)			
6	Si–Si	2.946		0.147
6	Cr–Cr	2.824		0.130
1	Cr–Si(1)	2.314		0.353
3	Cr–Si(2)	2.423	0.302	
3	Cr–Si(3)	2.576	0.190	
	Cr–Si(av)	2.473	0.261	
	CrSi in VP-Type Structure			
6	Si–Si	3.180		0.060
6	Cr–Si	2.407		0.356
2	Cr–Cr(1)	3.112		0.061
6	Cr–Cr(2)	3.180		0.054
	CrSi in MnAl-Type Structure			
8	Cr–Si	2.641		0.205
6	Cr–Cr	3.050		0.075
6	Si–Si	3.050		0.124

[a] N is the number of equivalent bonds at each unique distance. [b] OP is the overlap population.

population in all of the bonds relative to the FeSi cell. The NiAs cells of VP and TiS thus appear to provide an environment where the possibilities for X–X overlap are quite small, and M–X overlap quite large. For TiS and VP the X–X interactions are net antibonding, which is consistent with a NiAs structure in which the X atoms are relatively far from each other, assuring that X-atom electrons accumulate in M–X bonding levels rather than X–X antibonding levels. Placing CrSi in the VP (NiAs) type structure, by contrast, prevents the net bonding Si–Si interactions from occurring to the extent they do in the FeSi structure, thereby reducing the total overlap population. The actual CrSi (FeSi) and MnAl (CsCl) structures thus provide environments permitting significant X–X bonding, while the VP (NiAs) structure is inconsistent with significant X–X bonding. As the electron count in the "X" element s- and p-levels increases, the X–X interactions become net antibonding and the crystal structure changes from the CsCl or FeSi type to the NiAs type to minimize X–X interaction.

The computed overlap population curves for CrSi in the observed FeSi structure and the MnAl (CsCl) cell showed only slight differences between these structures, with the observed structure having higher total overlap. These results do tend to support the FeSi-type structure as the preferred structure for CrSi, in contrast with the results of Pettifor and Podloucky.[9] As suggested by these authors, this may be the result of their neglect of s-electrons.

The present study was motivated largely by a desire to understand the trends in atomization enthalpies presented in Figures 1 and 2. It has already been noted that the computed overlap population in the M–X bond (excluding other bond overlap populations) appears to correlate with the experimental atomization heats to ground-state atoms presented in Figure 1. It is not, however, completely obvious why there should be such a correlation, since, in atomizing a solid, all of the bonds (M–M, M–X, and X–X) must be broken. One might therefore suspect that the atomization heat, particularly to valence state atoms, would vary across the compound series in parallel with the *total* overlap population per primitive cell, appropriately weighted and summed over different bond types, as displayed in Figure 3. However, mixed valence states must be allowed for, as noted earlier.

The question of the preferred valence state for the "X" elements was raised in connection with Figure 2. The orbital occupancies for the X element tabulated in Table IV can be written as a linear combination of s^2p^{n-2} and sp^{n-1} configurations, and a percentage contribution of each configuration can be determined. These percentages are certainly not absolute, in part because of the arbitrary way the overlap charges are divided between atoms in the Mulliken population analysis. The results indicate that Al in MnAl leans heavily (71%) toward an sp^2 configuration, while Si in CrSi is about 49% sp^3. If the computed electron occupancies are used as a guide to determine what fraction of a spectroscopic promotion energy should be added to the experimental atomization heats, the sequence of atomization heats to "valence" state atoms becomes TiS < VP < MnAl < CrSi, exactly parallel to the total overlap population per primitive cell in the solid.

Conclusion

The electronic structures of the 10-electron series of binary compounds MnAl–CrSi–VP–TiS (MnAl is actually within a broad single-phase region) have been investigated using an extended Hückel calculational approach. The results, particularly the variations of overlap population in the different bonds, help provide an understanding of the changes in atomization enthalpy and crystal structure across the series. The calculations show a change in the manner in which the p-block element uses its s-electrons in bonding, and this change correlates with a change in preferred crystal structure. In TiS and VP, with the NiAs-type structure, the bonding is dominated by M–X interactions, whereas in CrSi and MnAl which have the FeSi-type and CsCl-type structures, respectively, X–X interactions are of increasing importance.

Acknowledgment. We thank Professor Roald Hoffmann for making his extended Hückel programs available to us. Helpful comments were made by Professors H. F. Franzen and Stephen Lee. This research was supported by the National Science Foundation, Grant No. DMR8721722.

Supplementary Material Available: Figures showing densities of states and l-decomposed densities of states (5 pages). Ordering information is given on any current masthead page.